

## Article

# Extraction of High-Purity Native State Gutta-Percha from Enzymatic Hydrolyzed *Eucommia ulmoides* Pericarps by Ultrasound Treatment and Surfactant Aqueous Phase Dispersion

Qili Shi <sup>1,2</sup>, Yangjie He <sup>1,2</sup>, Xuejun Zhang <sup>1,2</sup>, Qiaoling Wu <sup>1,2</sup> and Han Tao <sup>1,2,\*</sup>

<sup>1</sup> School of Liquor and Food Engineering, Guizhou University, Guiyang 550025, China; shiqilijayou@163.com (Q.S.); heyj994@163.com (Y.H.); xjzhang@gzu.edu.cn (X.Z.); wql9695@163.com (Q.W.)

<sup>2</sup> Key Laboratory of Fermentation Engineering and Biopharmacy of Guizhou Province, Guizhou University, Guiyang 550025, China

\* Correspondence: htiao@gzu.edu.cn; Tel.: +86-0851-88236895

**Abstract:** Herein, a method of ultrasound treatment combined with surfactant aqueous phase dispersion was proposed for the extraction of high-purity gutta-percha in its native state from enzymatic hydrolyzed *Eucommia ulmoides* pericarps. Firstly, the plant tissues wrapped around gutta-percha were destructed through enzymatic hydrolysis, then the plant tissues debris still attached to gutta-percha were further stripped off by ultrasound. Finally, under the “amphiphilic” action of sodium dodecyl sulfate (SDS), the entangled gutta-percha was untwined, allowing the residual plant tissue debris to be released and precipitated, thus high purity gutta-percha was obtained. The process parameters were optimized through single factor and response surface experiments. The optimal parameters for ultrasonic treatment were displayed as follows: frequency of 40 kHz, power of 320 W, time of 7.3 h, temperature of 50 °C, and material-to-liquid ratio of 1:70 g/mL, and for the aqueous phase dispersion of surfactant were SDS concentration 1.7%, temperature 80 °C, stirring speed 1200 rpm, solid-to-liquid ratio 1:60 g/mL, and time 60 h. Under optimal conditions, the purity of gutta-percha reached  $95.4 \pm 0.31\%$  and its weight average molecular weight ( $M_w$ ) was  $20.85 \times 10^4$ . Moreover, the obtained gutta-percha maintained its native filamentous form. The obtained products were characterized by IR, NMR, XRD, TGA, DSC, and tensile experiments, which showed that the obtained product was gutta-percha and maintained the natural  $\alpha$ - and  $\beta$ - crystal structure. The proposed method overcomes the disadvantages of the traditional organic solvent method, which has great environmental pollution and destroys the gutta-percha structure. This is also the first reported method to obtain high purity gutta-percha while maintaining its native state.

**Keywords:** native state gutta-percha; ultrasound; surfactant aqueous dispersion; enzymatic hydrolysis; *Eucommia ulmoides* pericarps



**Citation:** Shi, Q.; He, Y.; Zhang, X.; Wu, Q.; Tao, H. Extraction of High-Purity Native State Gutta-Percha from Enzymatic Hydrolyzed *Eucommia ulmoides* Pericarps by Ultrasound Treatment and Surfactant Aqueous Phase Dispersion. *Agriculture* **2022**, *12*, 904. <https://doi.org/10.3390/agriculture12070904>

Academic Editors: Kristian Wende, Zdenek Wimmer and William N. Setzer

Received: 28 April 2022

Accepted: 17 June 2022

Published: 21 June 2022

**Publisher's Note:** MDPI stays neutral with regard to jurisdictional claims in published maps and institutional affiliations.



**Copyright:** © 2022 by the authors. Licensee MDPI, Basel, Switzerland. This article is an open access article distributed under the terms and conditions of the Creative Commons Attribution (CC BY) license (<https://creativecommons.org/licenses/by/4.0/>).

## 1. Introduction

*Eucommia ulmoides* Oliv (*E. ulmoides*) is a peculiar, rare tree species in China. Its leaves, bark, and samara all contain gutta-percha [1], commonly known as balata rubber (Figure 1). Gutta-percha is a white filamentous high-molecular polymer with the structural formula of *trans*-1,4-polyisoprene, which is the isomer of natural hevea rubber [2]. Therefore, gutta-percha is the best substitute and supplement for hevea rubber with considerable development potential [3,4].

Besides, gutta-percha can be applied in many fields such as the rubber industry, chemical industry [5], medical [6], and sports [7] due to its rubber-plastic dual characteristics [8,9], good anti-acid and anti-alkaline properties, tear resistance and shape memory function [10]. Meanwhile, gutta-percha is also an ideal ergonomic material, which can be used to prepare artificial blood vessels and skin, etc. [6,11]. However, the research and application of gutta-percha mostly rest in the laboratory stage at present, without large-scale research or

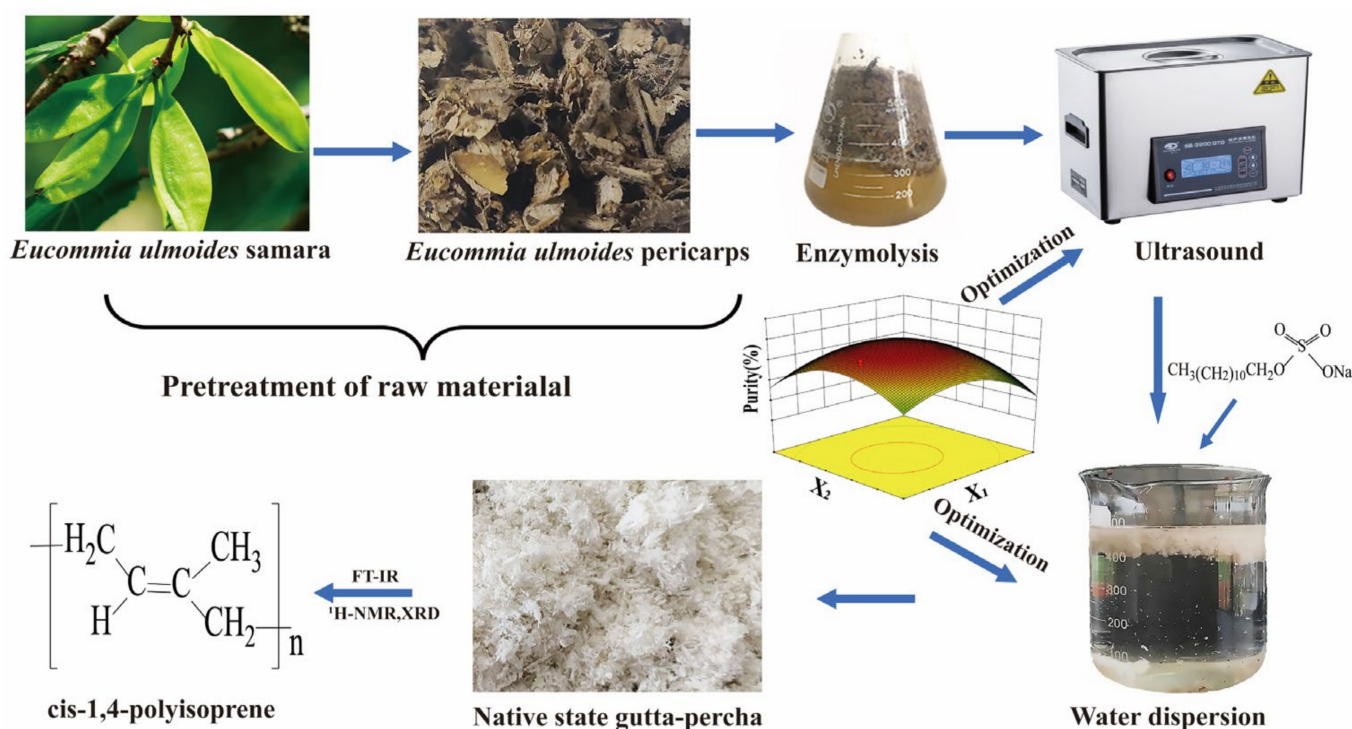
industrialized application. The key reason lies in the lack of a high-quality and high-purity gutta-percha extraction technology.



**Figure 1.** Gutta-percha in different *E. ulmoides* tissues. (a) leaves, (b) bark and (c) samara.

So far, the reported gutta-percha extraction methods include mechanical crushing, organic solvent extraction, steam explosion, microbial fermentation, and enzymatic hydrolysis method [12–14]. Among them, the enzymatic hydrolysis method was first proposed by our laboratory [15], which utilizes the biocatalytic action of appropriate enzymes to degrade the plant tissues wrapped around gutta-percha, thus achieving the separation of gutta-percha from the plant tissues. Compared with other methods, enzymatic hydrolysis uses enzymes to specifically degrade plant tissues under mild conditions, so that the natural structure of gutta-percha and the physiological activity of the medicinal components in *Eucommia* are maintained at the same time, thus allowing for the simultaneous extraction of gutta-percha and natural medicinal components, and enabling the production costs of gutta-percha to be reduced. However, due to the complexity of plant tissue components, the plant tissues cannot be completely removed so far just by the enzymatic hydrolysis alone. Gutta-percha products after enzymatic hydrolysis still contain many plant tissue debris. Hence, it is necessary to combine other technologies to continuously remove the remaining plant tissue debris.

In this study, the ultrasonic treatment combined with surfactant aqueous phase dispersion was proposed for the first time to further purify gutta-percha from enzymatic hydrolyzed *E. ulmoides* pericarps. The adhesive force between the gutta-percha and the residual plant tissues was weakened by ultrasound. Next, the intertwined gutta-percha was untwined under the “amphiphilic” action of surfactants. Subsequently, the relieved plant tissue debris sank to the bottom, while gutta-percha floated to the water surface, thus obtaining gutta-percha with high purity (>95%) in a pollution-free way. The extraction scheme is shown in Scheme 1.



**Scheme 1.** Illustration of gutta-percha extraction process.

## 2. Materials and Methods

### 2.1. Materials

*E. ulmoides* pericarps obtained by mechanical de-seeding of *Eucommia* samara was provided by Zhejiang Xuyuan *Eucommia* Biotechnology Co. Ltd. (Jiaxing, China). Cellulase (ZH-1) was purchased from Daheng Biotechnology Company (Zhangjiagang, China). The special enzymes for paper pulping, MTPE-90, and OCE-90, were purchased from Sukohan Biological Engineering Co. Ltd. (Weifang, China). 4.0 g/L complex enzyme solution was obtained by adding appropriate amounts of ZH-1, OCE-90, and MTPE-90 (mass ratio 1:1:1) to 1000 mL of citric acid-sodium citrate buffer at pH 6.0, stirred at 50 °C for 30 min and then filtered. Polyethylene glycol octylphenyl ether (S1), polyoxyethylene lauryl ether (S2), polyethylene glycol PEG-400 (S3), dioctyl sodium sulfosuccinate (S4), alkylphenol polyoxyethylene ether (S5), fatty alcohol polyoxyethylene ether (S6), sodium dodecyl sulfate (S7), hexadecyltrimethylammonium bromide (S8), octadecyl dimethyl ammonium chloride (S9) were purchased from De-Zhong Chemical Technology Co. Ltd. (Foshan, China).

### 2.2. Enzymatic Pretreatment of Raw Materials

The *E. ulmoides* pericarps obtained by mechanical de-seeding of *Eucommia* samara were used as raw material, which was ultrasonicated for 8 h in water and then dried at 60 °C under vacuum. After that, 10 g of the above treated *E. ulmoides* pericarps were accurately weighed and put into a triangular flask, 300 mL of 4.0 mg/mL complex enzyme solution was added and the enzymatic hydrolysis was carried out at 50 °C for 4 h. The enzymatic solution was filtered. The solids were collected and washed repeatedly with water and dried under a vacuum at 60 °C to obtain the enzymatic hydrolyzed *E. ulmoides* pericarps.

### 2.3. Ultrasonic Treatment of Enzymatic Hydrolyzed *E. ulmoides* Pericarps

5.0 g of enzymatically hydrolyzed *E. ulmoides* pericarps were sonicated in water for a certain time, the solids were collected and dried under vacuum at 60 °C to obtain crude gutta-percha. Five experimental factors (material-to-liquid ratio, sonication frequency, sonication power, sonication temperature, and sonication time) were optimized by single-

factor experiments. Based on the results of a single-factor test, the factors were further optimized by the Box-Behnken Design (BBD) with gutta-percha purity as the index, and the levels of experimental factors are shown in Table 1.

**Table 1.** Codes and levels of independent variables for response surface analysis during ultrasonication.

Level	Factors				
	X <sub>1</sub> Frequency kHz	X <sub>2</sub> Power W	X <sub>3</sub> Time h	X <sub>4</sub> Temperature °C	X <sub>5</sub> Material-to-Liquid Ratio g/mL
−1	33	280	4	40	1:60
0	40	320	6	50	1:70
1	59	360	8	60	1:80

#### 2.4. Purification of Crude Gutta-Percha

10.0 g of crude gum was weighed accurately, stirred magnetically at a certain temperature for a certain time in an aqueous solution containing surfactant, then the solid was collected, washed several times with double distilled water to remove residual surfactant and dried under vacuum at 60 °C to obtain gutta-percha.

Six experimental factors (surfactant type, surfactant concentration, water bath temperature, water bath time, stirring rate, and material-to-liquid ratio) affecting the purification of gutta-percha were investigated. According to the single factor test results, the surfactant was fixed as S7, and BBD was used to optimize the experimental factors with gutta-percha purity as the index, the factors and levels are shown in Table 2.

**Table 2.** Codes and levels of independent variables during surfactant aqueous phase dispersion.

Level	Factors				
	X' <sub>1</sub> Concentration %	X' <sub>2</sub> Temperature °C	X' <sub>3</sub> Time h	X' <sub>4</sub> Stirring Speed rpm	X' <sub>5</sub> Material-to-Liquid Ratio g/mL
−1	1	80	40	800	1:40
0	2	85	50	1200	1:50
1	3	90	60	1600	1:60

#### 2.5. Determination of Gutta-Percha Purity

M<sub>0</sub> g of gutta-percha was weighed accurately and placed in a triangular flask, then 200 mL of mixed xylene containing 0.25% of 2-thiolybenzothiazole was added. The gutta-percha was fully dissolved by heating to 125~130 °C and then the hot solution was filtered by a clean and dry stainless steel mesh sieve (45 μm pore size) with known mass. The residual impurities in the triangular flask were also washed into the mesh sieve with hot solvent. Subsequently, the sieve containing impurities was washed twice with petroleum ether and dried to a constant weight. The purity of gutta-percha can be calculated according to the following formula.

$$Y = \left(1 - \frac{M_2 - M_1}{M_0}\right) \times 100\% \quad (1)$$

where, M<sub>0</sub> (g) is the weight of the gutta-percha, M<sub>1</sub> (g) is the weight of the mesh sieve and M<sub>2</sub> (g) is the total weight of the mesh sieve and impurities.

#### 2.6. Identification and Characterization of Gutta-Percha

Fourier transform infrared (FT-IR) spectra were collected on an IRAffinity-1S FT-IR spectrometer (Shimadzu, Kyoto, Japan). Gutta-percha was dissolved with petroleum ether and then evenly coated on KBr tablets. The <sup>1</sup>H-NMR spectra were collected using AVANCE III 500 MHz nuclear magnetic resonance spectrometer (Bruker, Fällanden, Switzerland) with CDCl<sub>3</sub> as the solvent and TMS as the internal standard (δ<sub>H</sub> = 0). X-ray Diffraction Analysis was performed with Empyrean X-ray Diffractometer (PANalytical B. V., Almelo,

The Netherlands). The  $2\theta$  angle range was  $5^{\circ}\sim 35^{\circ}$ . Gel permeation chromatography (GPC) analysis was carried out on a Waters GPC system including a Plgel 5  $\mu\text{m}$  MIXED-C column (Agilent Technologies Co., Ltd., Beijing, China).  $\text{CHCl}_3$  was used as the mobile phase at a flow rate of 1 mL/min. STA 449 F5 Thermogravimetric analyzer (NETZSCH, Selb, Germany) was used for Thermo gravimetric (TGA) analysis in the range of  $28\sim 600^{\circ}\text{C}$ . Tensile tests were performed using CMT5304 (Sansi, Shenzhen, China) at room temperature. DSC analysis was performed with a TA Q2000 DSC instrument (TA, New Castle, DE, USA), and the scanning temperature was  $-75^{\circ}\text{C}\sim 125^{\circ}\text{C}$ .

### 2.7. Data Processing and Analysis

Excel 2019 was used to process the data and Origin 8.5 (Northampton, MA, USA) was used for graphical plotting. Box-Behnken response surface experimental design, ANOVA, and significant difference analysis were performed by Design-Expert 8.0.6 (Minneapolis, MN, USA). FT-IR was analyzed by OMNIC software 8.2 (Madison, WI, USA) and  $^1\text{H-NMR}$  spectra was analyzed by MestReNova software 12.0.1 (Santiago de Compostela, Spain).

## 3. Results

### 3.1. Enzymatic Hydrolysis of *E. ulmoides* Pericarps

Gutta-percha grows in *E. ulmoides* and is wrapped by complex plant tissues (the main components are cellulose, pectin, and lignin). Gutta-percha can be released to some extent by destroying the plant tissues outside gutta-percha through the degradation of specific enzymes. Figure 2 compares the *E. ulmoides* pericarps before and after enzymatic hydrolysis. It can be observed that after enzymatic hydrolysis, the plant tissues wrapped at the outer layer of gutta-percha were pertinently degraded to a great extent, so gutta-percha was exposed. In addition, it can be seen from Figure 2c that gutta-percha still kept its original filamentous state after enzymatic pretreatment. However, a lot of plant residues were still wrapped in the enzymatically hydrolyzed *E. ulmoides* pericarps. Hence, the plant residues were required to be further removed.

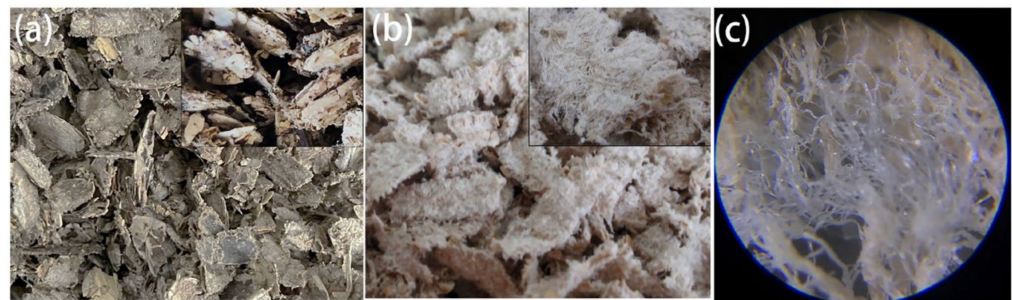


**Figure 2.** Photographs of *E. ulmoides* pericarps before and after enzymatic hydrolysis. (a) before, (b) after, (c) optical micrograph of gutta-percha in enzymatic hydrolyzed *E. ulmoides* pericarps ( $\times 100$ ).

### 3.2. Ultrasonic Stripping of Plant Tissue Debris

The adhesive force between gutta-percha and the plant debris can be weakened by the cavitation effect of ultrasound, thus enabling the debris to be stripped from the gutta-percha, the corresponding mechanism of which was discussed in the Supplementary Materials (Scheme S1).

#### 3.2.1. Single-Factor Optimization of Ultrasonic Experimental Parameters

The ultrasonic experimental parameters were optimized using gutta-percha purity as the index, and the results are shown in Figure 3. The influence of ultrasonic frequency was shown in Figure 3a. The results showed that the purification effect was the best at 40 kHz, and then weakened at 59 kHz. A possible reason for this is that too high frequencies lead to the attenuation of ultrasonic vibrations, which weakens the cavitation intensity. The influence of ultrasonic power was shown in Figure 3b. As the power was elevated, the

ultrasound energy increased, which was good for stripping off plant debris. The purity of gutta-percha was the highest at 320 W. However, the purity was reduced if the power was continuously increased, indicating that the separation of gutta-percha was not further promoted by continuously increasing the ultrasonic power, and excessive ultrasonic power would also increase the energy consumption. As shown in Figure 3c, the purity increased with increasing sonication time, but after 6 h, the purity changed very little. Considering the time cost, the sonication time of 6 h was chosen. The influence of ultrasonic temperature on the purity is exhibited in Figure 3d. The purity was the highest (60.5%) at 50 °C. As the temperature was further elevated, the purity declined, since excessive temperature resulted in the decline of impact force of cavitation microbubbles. The material-to-liquid ratio was also optimized (Figure 3e). In the range of 1:50 g/mL to 1:70 g/mL, the purity increased with the increase of material-to-liquid ratio, but further decreased, which was possibly due to the thermal effect, mechanical effect, and cavitation effect of ultrasonic waves on unit volume of extraction solution being weakened when the material-to-liquid ratio was too large [16,17]. According to the results in Figure 3, the optimization central points for BBD of frequency, power, time, temperature, and material-to-liquid ratio were 40 kHz, 320 W, 6 h, 50 °C, and 1:70 g/mL, respectively.

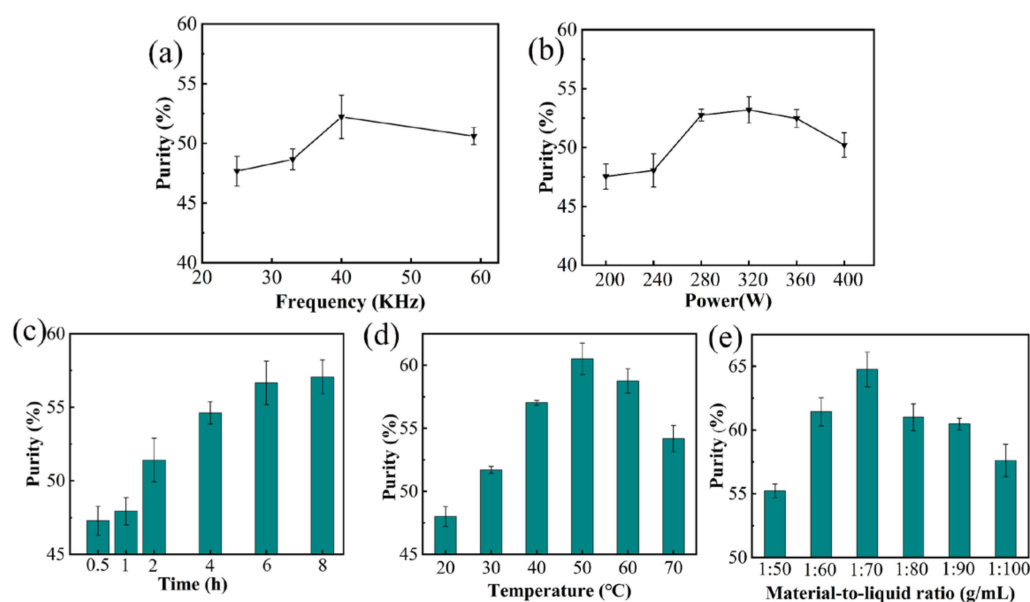


**Figure 3.** Effect of different ultrasonic parameters on the purity of gutta-percha. (a) frequency, (b) power, (c) time, (d) temperature, (e) material-to-liquid ratio.

### 3.2.2. BBD Optimization and Verification of Ultrasonic Parameters

Forty-six groups' tests of 5-factor at 3-level were designed based on the principle of BBD, and the results are listed in Table S1. The multiple regression analysis was performed to obtain the following regression equation:

$$Y = 66.12 + 0.73X_1 + 1.65X_2 + 3.37X_3 + 1.70X_4 + 0.78X_5 + 0.59X_1X_2 + 0.34X_1X_3 - 1.45X_1X_4 - 0.20X_1X_5 + 1.05X_2X_3 + 1.71X_2X_4 - 0.54X_2X_5 - 0.39X_3X_4 - 0.85X_3X_5 - 0.91X_4X_5 - 6.94X_1^2 - 5.77X_2^2 - 4.51X_3^2 - 3.84X_4^2 - 3.52X_5^2 \quad (2)$$

ANOVA results were listed in Table S2. The  $p$ -value ( $<0.0001$ ) suggests that the model is significant. The coefficient of determination ( $R^2$ ) was 0.9655, indicating that this model could explain 96.55% of the variation in response values. The  $p$ -value of lack-of-fit was not significant ( $0.1499 > 0.05$ ), indicating that the regression model adequately reflected the actual situation. It can also be seen from Table S2 that the one-order term ( $X_2$ ,  $X_3$ ,  $X_4$ ), the quadratic term ( $X_1^2$ ,  $X_2^2$ ,  $X_3^2$ ,  $X_4^2$ ,  $X_5^2$ ), and the interaction term ( $X_1X_4$ ,  $X_2X_4$ ) exerted extremely significant influences on gutta-percha purity ( $p < 0.01$ ). the one-order

term ( $X_1$  and  $X_5$ ) had a significant effect on gutta-percha purity ( $p < 0.05$ ). According to the F value, the influences of different factors on gutta-percha purity were sorted as: Time > Temperature > Power > Frequency > Material-to-liquid ratio.

To visualize the effect of the interaction between the ultrasonic factors on  $Y$ , the 3D surface charts were drawn (Figure 4) [18]. The steeper surface and the higher slope indicate a stronger influence of the interaction between two factors on gutta-percha purity [19]. It could be observed that the interaction between frequency ( $X_1$ ) and temperature ( $X_4$ ) and that between power ( $X_2$ ) and temperature ( $X_4$ ) had greater impacts on the removal of plant tissue fragments.

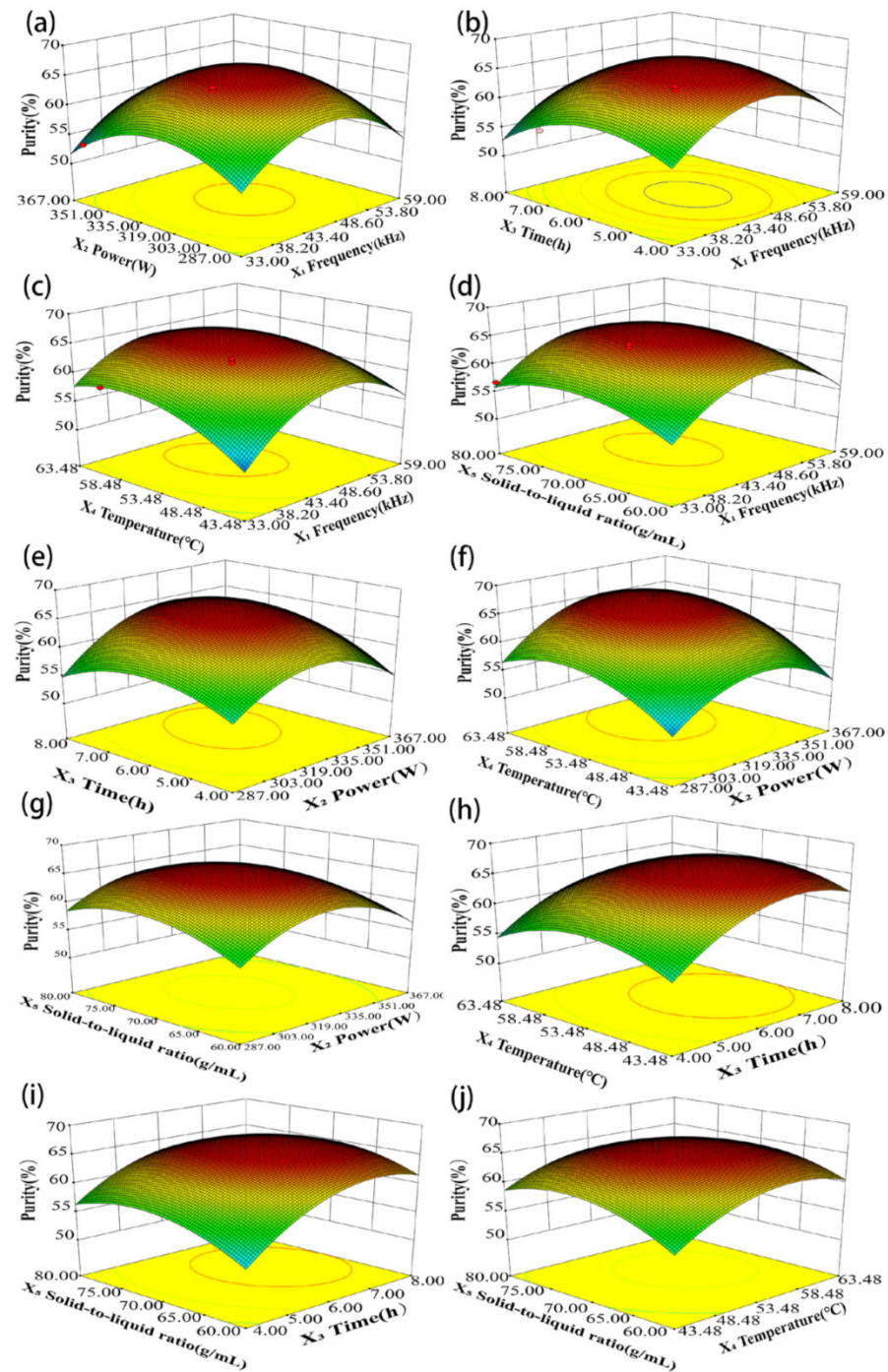


**Figure 4.** 3D response surface curves of interactive effects between different ultrasonic factors. (a)  $X_1X_2$ , (b)  $X_1X_3$ , (c)  $X_1X_4$ , (d)  $X_1X_5$ , (e)  $X_2X_3$ , (f)  $X_2X_4$ , (g)  $X_2X_5$ , (h)  $X_3X_4$ , (i)  $X_3X_5$ , (j)  $X_4X_5$ . ( $X_1$ , frequency;  $X_2$ , power;  $X_3$ , time;  $X_4$ , temperature;  $X_5$ , material-to-liquid ratio).

The optimal ultrasonic experimental parameters predicted through BBD were frequency 44.83 kHz, power 325.33 W, time 7.31 h, temperature 49.28 °C, and material-to-liquid ratio 1: 66.73 g/mL. Under such conditions, the predicted purity was 65.9%. Three parallel validation tests were carried out at 40 kHz, 320 W, 7.3 h, 50 °C, and 1:70 g/mL. The purity of the obtained gutta-percha was  $64.8 \pm 0.55\%$ , which only deviated slightly from the predicted value, thus indicating the reasonability and reliability of the constructed model.

The morphology of the crude gutta-percha obtained after ultrasonic treatment is presented in Figure 5a. It can be observed that the adhesion of the plant tissue debris to the gutta-percha became looser after sonication, and the amount of debris wrapped in the crude gutta-percha was obviously reduced. Figure 5b shows that the gutta-percha still remained in the filamentous state after sonication.

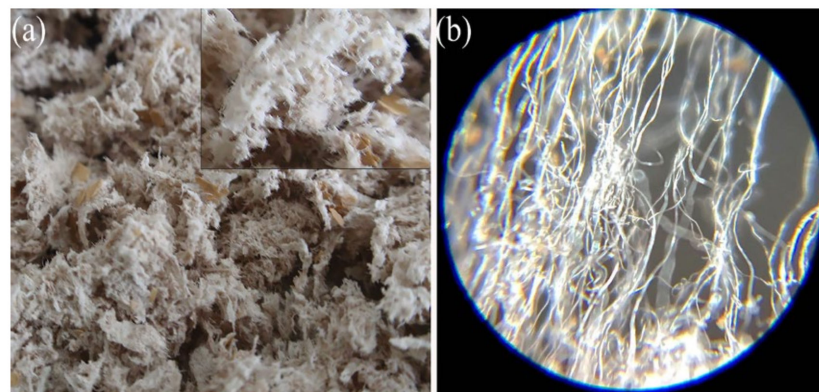


**Figure 5.** (a) Photograph of crude gutta-percha obtained after ultrasonic treatment and (b) optical micrograph of gutta-percha ( $\times 100$ ).

### 3.3. Purification of Crude Gutta-Percha

Under the “amphiphilic” action of surfactant, the entangled gutta-percha unentangled and released the plant tissue residues wrapped in gutta-percha. The related mechanism was discussed in the supplementary material (Figure S1).

#### 3.3.1. Single-Factor Optimization of Surfactant Dispersion Conditions

The effect of the aqueous phase dispersion conditions on gutta-percha purity is shown in Figure 6. First, the surfactant species were chosen (Figure 6a). It was found that SDS (S-7) had the best effect with a purity of 84.4%. SDS is an anionic surfactant with superior wettability and permeability and is inexpensive. Therefore, SDS was chosen in the subsequent experiments.

Next, the influence of SDS concentration on purity was explored (Figure 6b). The results showed that the purity tended to increase in the concentration range of 0.5 to 2.0%, and reached 85.0% at 2.0%. As the concentration was further increased, the purity decreased, probably due to the formation of too dense micelles, which were detrimental to the dispersion of gutta-percha.

The effect of temperature on the purification of gutta-percha is exhibited in Figure 6c. The purity of gutta-percha reached a maximum (86.4%) at 85 °C.

The influence of extraction time is displayed in Figure 6d. As the time was lengthened, SDS exerted a more sufficient effect, and the purity showed a rising trend. The purity increased to 87.8% at 50 h, but it was almost unchanged after then. Considering the time cost, the extraction time was chosen as 50 h for the subsequent experiment.

The influence of agitating rate is as shown in Figure 6e. As the agitating rate increased, the purity was enhanced, reaching 93.6% at 1200 rpm. When the stirring speed was further accelerated, the purity declined, which might be related to the fact that the too fast agitation was not good for the stability of micelles. Besides, it could be found from Figure 6f that the purity was the highest (94.7%) at the material-to-liquid ratio of 1:50 g/mL.

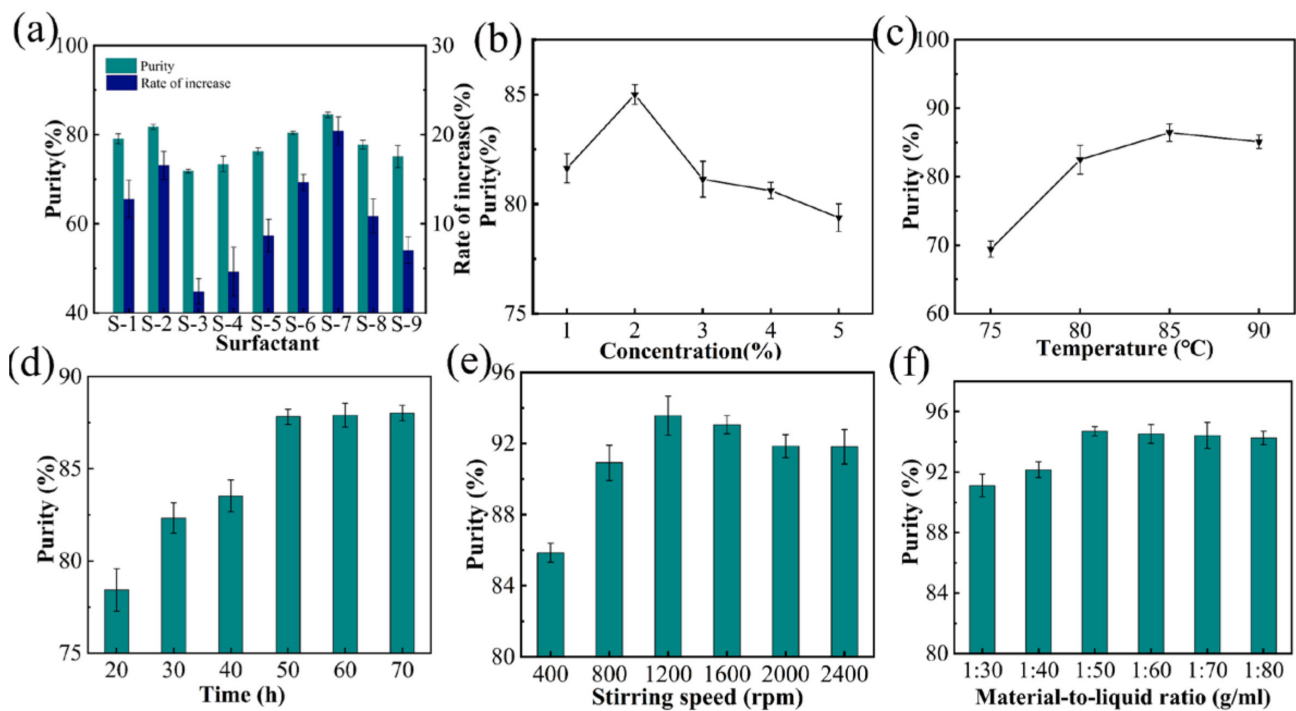


**Figure 6.** Effect of different dispersion conditions on gutta-percha purification. (a) surfactant species, (b) surfactant concentration, (c) temperature, (d) time, (e) stirring speed, (f) material-to-liquid ratio.

### 3.3.2. BBD-Based Optimization of Surfactant Dispersion Conditions and Verification

Based on the preliminary experimental results, 46 groups' tests of five independent variables at three levels were designed. The experimental results are displayed in Table S3. The experimental data were fitted by multi-regression analysis to obtain the following second-order polynomial equation:

$$Y = 94.71 + 1.47X'_1 + 0.88X'_2 + 3.58X'_3 + 1.90X'_4 - 0.56X'_5 + 1.16X'_1X'_2 + 0.21X'_1X'_3 + 0.77X'_1X'_4 - 0.44X'_1X'_5 - 4.49X'_2X'_3 + 0.18X'_2X'_4 - 0.06X'_2X'_5 - 3.04X'_3X'_4 - 1.96X'_3X'_5 - 0.42X'_4X'_5 - 4.13X'^2_1 - 3.21X'^2_2 - 4.65X'^2_3 - 3.53X'^2_4 - 0.94X'^2_5 \quad (3)$$

The ANOVA of the experimental results were presented in Table S4. The  $p$ -value of the model is  $<0.0001$ , indicating that the regression model is highly significant. the coefficient of determination ( $R^2$ ) was 0.9529, indicating that this model could explain 95% of the variation in response values. The  $p$ -value of lack-of-fit was insignificant ( $0.0567 > 0.05$ ), manifesting that the actual situation could be reflected by the regression model.

The one-order term ( $X'_1, X'_3, X'_4$ ), quadratic term ( $X'^2_1, X'^2_2, X'^2_3, X'^2_4$ ), and interaction term ( $X'_2X'_3, X'_3X'_4, X'_3X'_5$ ) in the regression model all generated extremely significant ( $p < 0.01$ ) influences on the purity of gutta-percha, the one-order term ( $X'_2$ ) and quadratic term ( $X'^2_5$ ) had a significant effect on gutta-percha purity ( $p < 0.05$ ). Meanwhile, it could be known from the  $F$  value that the influences of different factors on the purity of gutta-percha were sorted as Time  $>$  Stirring speed  $>$  Concentration  $>$  Temperature  $>$  Material-to-liquid ratio. The response surface plots were presented in Figure 7 [18]. It can be seen that the interaction between temperature ( $X'_2$ ) and time ( $X'_3$ ) and between time ( $X'_3$ ) and stirring speed ( $X'_4$ ) has greater effect on the purity of gutta-percha.

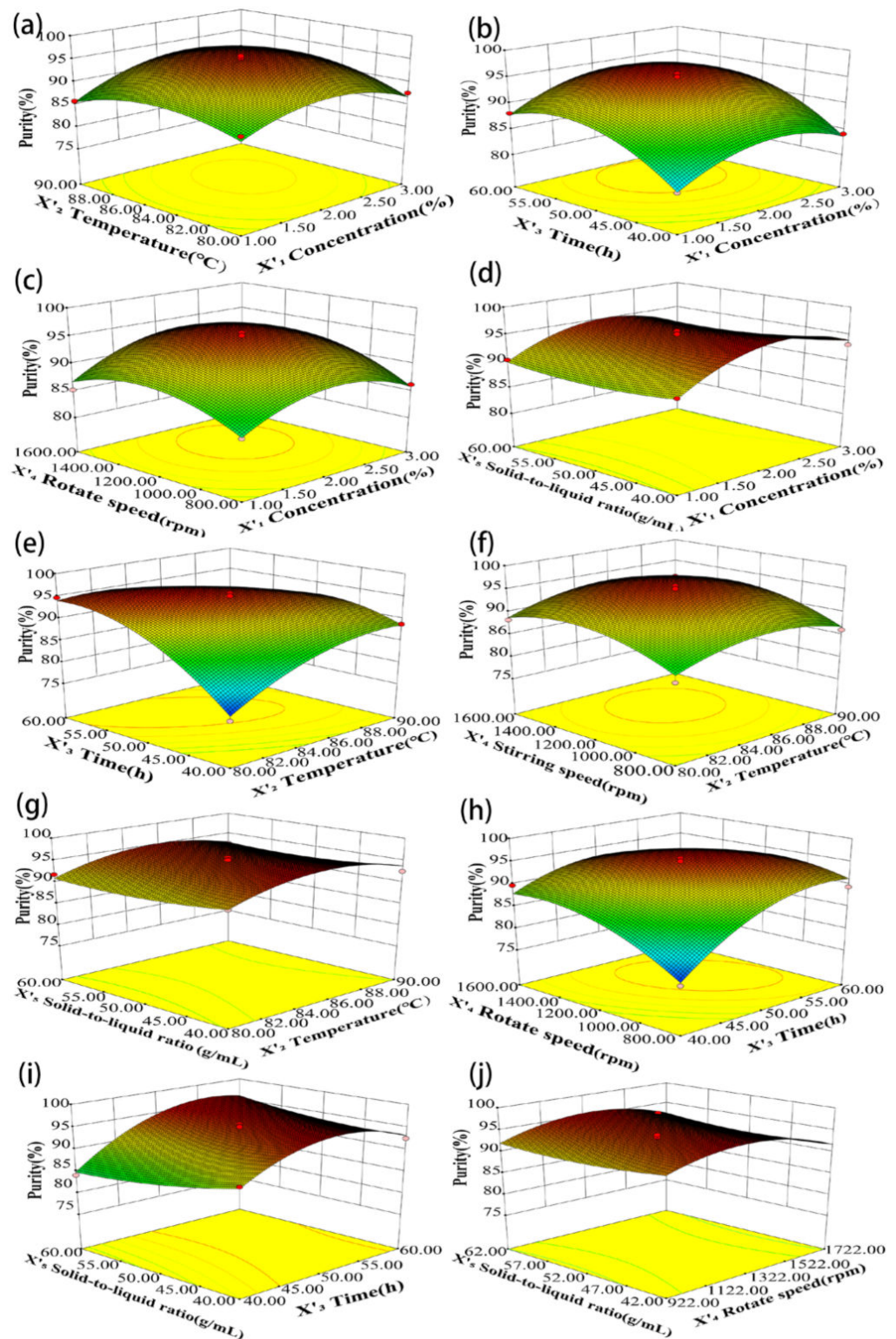


**Figure 7.** 3D response surface curves of interactive effects between different aqueous phase dispersion factors. (a)  $X'_1X'_2$ , (b)  $X'_1X'_3$ , (c)  $X'_1X'_4$ , (d)  $X'_1X'_5$ , (e)  $X'_2X'_3$ , (f)  $X'_2X'_4$ , (g)  $X'_2X'_5$ , (h)  $X'_3X'_4$ , (i)  $X'_3X'_5$ , (j)  $X'_4X'_5$ . ( $X'_1$ , concentration;  $X'_2$ , temperature;  $X'_3$ , time;  $X'_4$ , stirring speed;  $X'_5$ , material-to-liquid ratio)

The optimal aqueous phase dispersion conditions predicted by BBD were concentration 1.69%, temperature 80.40 °C, time 59.94 h, stirring speed 1120.94 rpm, and material-to-liquid ratio 1:58.96 g/mL, under which the predicted purity of gutta-percha was 95.8%.

The verification experiments were performed under practical experimental conditions (concentration 1.7%, temperature: 80 °C, time 60 h, stirring speed 1200 rpm, and material-to-liquid ratio 1:60 g/mL), and the purity of gutta-percha was  $95.4 \pm 0.31\%$ , which was approximate to the predicted value, thus proving the reasonability and reliability of the constructed model. Figure 8 shows the gutta-percha obtained after surfactant treatment. It can be seen that the purity of the gutta-percha was significantly improved, only very few impurities existed in the obtained gutta-percha. The gutta-percha still remained in its native filamentous state. Figure 8e also shows gutta-percha prepared by extraction with petroleum ether. It can be seen that the gutta-percha obtained is in the form of lumps and the natural morphology of gutta-percha has been destroyed.

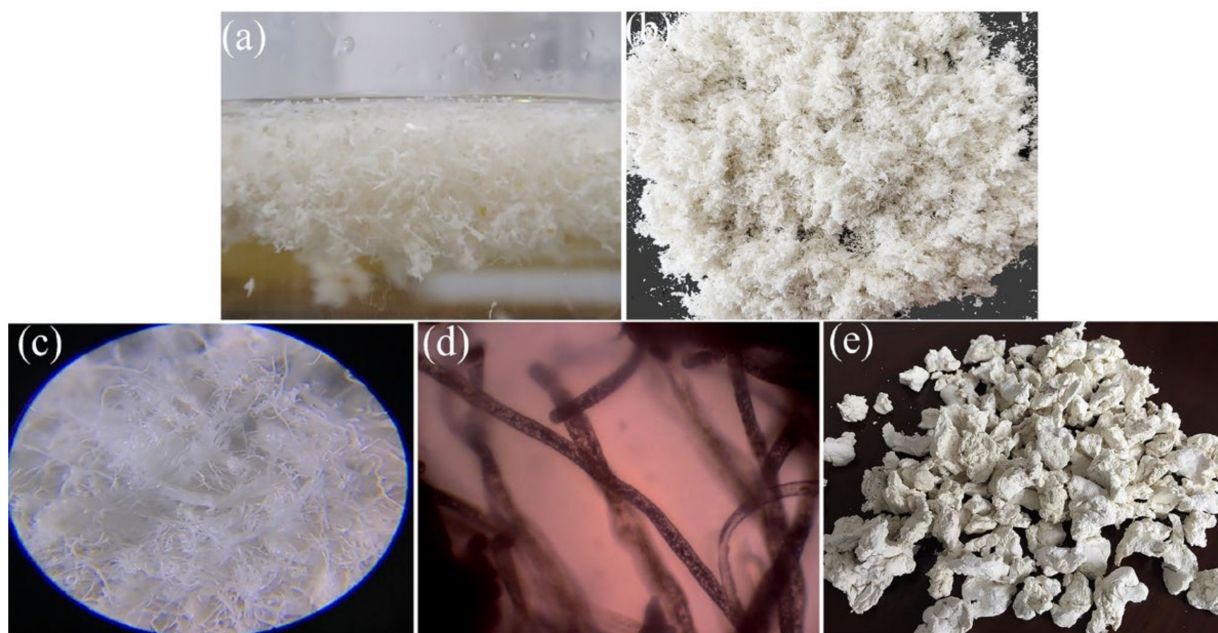


**Figure 8.** (a) gutta-percha dispersed in water, (b) gutta-percha after drying, (c) optical micrograph of gutta-percha  $\times 100$ , (d) optical micrograph of gutta-percha  $\times 400$ , (e) gutta-percha obtained by petroleum ether extraction.

### 3.4. Identification and Characterization of the Extracted Gutta-Percha

#### 3.4.1. Identification of Molecular Structure

FT-IR spectroscopy and  $^1\text{H-NMR}$  spectrum were used to identify the molecular structure of the obtained gutta-percha (Figure 9). In Figure 9a, the asymmetric stretching vibration peak of  $-\text{CH}_3$  was observed at  $2965\text{ cm}^{-1}$ , and the peaks at  $2912\text{ cm}^{-1}$  and  $2847\text{ cm}^{-1}$  correspond to the asymmetric stretching vibration and symmetric stretching vibration of  $-\text{CH}_2-$ , respectively. The symmetric and asymmetric deformation vibration peaks of  $-\text{CH}_3$  occurred at  $1383\text{ cm}^{-1}$  and  $1445\text{ cm}^{-1}$ , respectively. Peaks at  $799\text{ cm}^{-1}$  and  $1664\text{ cm}^{-1}$  are characteristic absorption peaks of the  $\text{trans-C}(\text{CH}_3)=\text{CH}-$  group, corresponding to the deformation vibration of C-H and the stretching vibration of C=C double bond, respectively. From the literature [20], the characteristic absorption peaks at 843, 910, and  $890\text{ cm}^{-1}$  in the IR spectra of polyisoprene are attributed to the 1,4-link, 1,2-link, and 3,4-link, respectively. In Figure 9a, only the absorption peak at  $843\text{ cm}^{-1}$  was found, indicating that the obtained gutta-percha has only 1,4-link. Figure 9a is in general agreement with previous literature [21,22] and shows the IR spectrum of *trans*-1,4-polyisoprene.

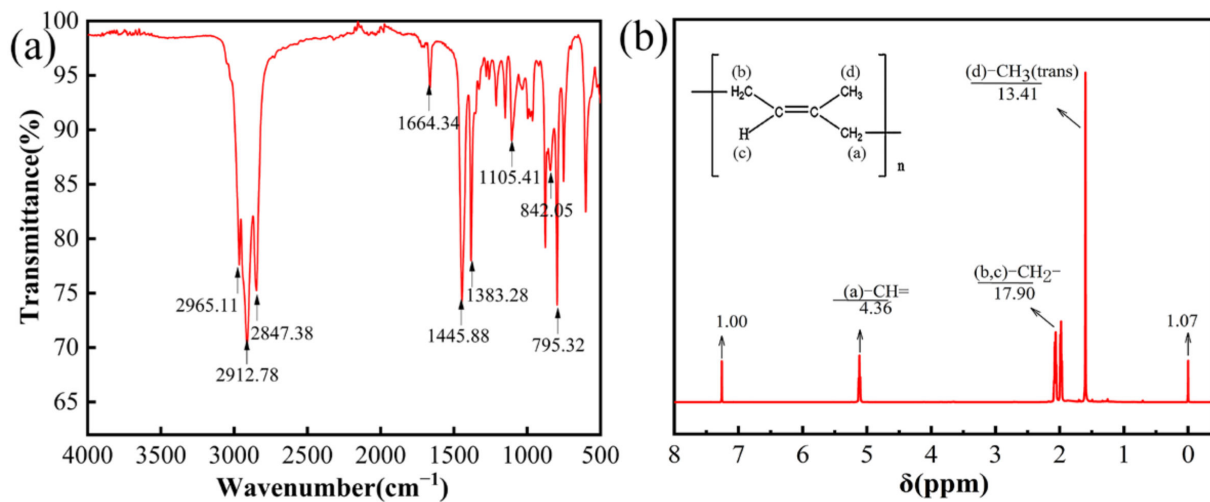


Figure 9. (a) FT-IR spectroscopy and (b)  $^1\text{H-NMR}$  spectrum of the extracted gutta-percha.

Figure 9b displays the NMR spectrum of the as-prepared gutta-percha. The peak signal is strong at chemical shift 1.60 ppm, which can be attributed to the methyl proton peak in the *trans*-1,4- structure, while the absence of the methyl proton peak in the *cis*-1,4- structure at chemical shift 1.67 ppm indicates the absence of *cis*-1,4 -polyisoprene [23,24]. The two peak signals at chemical shifts of 2.06 ppm and 1.96 ppm correspond to two methylene proton absorption peaks. In addition, the peak at 5.12 ppm is the characteristic peak of the unsaturated proton on the C=C double bond in the *trans*-1,4- structure. No signal peaks for protons in the 1,2-structure and 3,4-structure were observed. In combination with the results in Figure 9a,b, the structure of the extracted gutta-percha was confirmed to be *trans*-1,4 polyisoprene [8].

### 3.4.2. XRD Analysis

There are two crystalline forms in gutta-percha [25,26], namely  $\alpha$ - and  $\beta$ -crystalline forms. As shown in Figure 10a, the peaks at  $11.4^\circ$ ,  $17.9^\circ$ ,  $26.9^\circ$ ,  $30.8^\circ$ , and  $33.5^\circ$  are the characteristic peaks of the  $\alpha$ -crystalline form of gutta-percha, while the peaks at  $19.1^\circ$  and  $22.8^\circ$  are the characteristic peaks of the  $\beta$ -crystalline form [27,28], showing that the extracted gutta-percha maintains its natural crystalline structure.

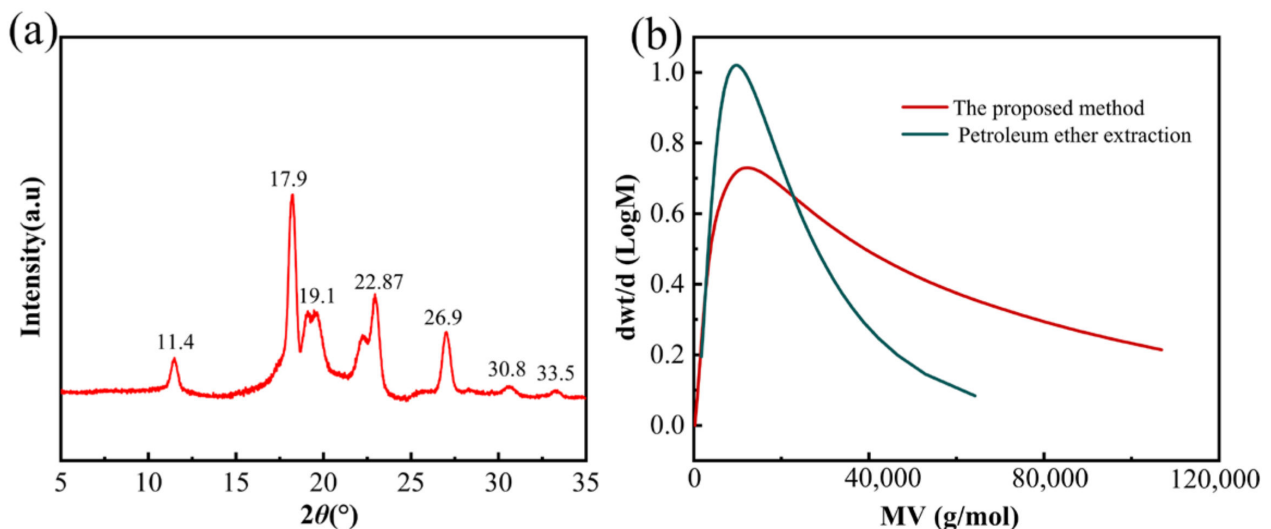


Figure 10. (a) XRD of the purified gutta-percha, (b) Molecular weight distribution curves of gutta-percha.

### 3.4.3. Analysis of Molecular Weight and Molecular Weight Distribution

The molecular weights and molecular weight distributions of the extracted gutta-percha were measured by GPC (Figure 10b). The weight-average molecular weight (Mw) and number-average molecular weight (Mn) of gutta-percha obtained by enzymatic hydrolysis combined with ultrasound treatment and surfactant aqueous phase dispersion were  $20.85 \times 10^4$  and  $5.37 \times 10^4$ , with a polydispersity index (Mw/Mn, PDI) of 3.88. Also, the Mw and Mn of gutta-percha extracted with petroleum ether were  $13.25 \times 10^4$  and  $5.88 \times 10^4$ , respectively, with a PDI of 1.91 (Table 3). It can be noted that the gutta-percha extracted by the proposed method has higher Mw than the traditional organic solvent method, indicating that the proposed method in this work better preserves the molecular structure of gutta-percha. PDI is an indicator to assess the distribution width of a polymer's molecular weight. Compared to petroleum ether extraction, the gutta-percha obtained by the proposed method has a wider molecular weight distribution, indicating that gutta-percha with smaller or larger molecular weights was also extracted efficiently. Moreover, the molecular weights and DPIs of gutta-percha in other reported literature are also listed in Table 3. It can be observed that the gutta-percha extracted by the proposed method has a higher molecular weight and broader molecular weight distribution. More importantly, the gutta-percha in this work maintained its natural filamentous form.

**Table 3.** Comparison of molecular weights and DPIs of gutta-percha extracted by different methods.

Method	Eucommia Organ	Mw ( $\times 10^4$ )	Mn ( $\times 10^4$ )	PDI	Ref.
Enzymatic pretreatment combined with ultrasound and surfactant aqueous phase dispersion	pericarps	20.85	5.37	3.88	This work
Petroleum ether extraction	pericarps	13.25	5.88	1.91	This work
Petroleum ether extraction	pericarps	5.6	5.1	1.1	[29]
Toluene extraction followed by ethanol purification	pericarps	8.4	3.9	2.18	[30]
Turpentine extraction	bark	4.9	1.9	2.54	[31]
Steam explosion followed by petroleum ether extraction	bark	20.46	12.64	2.2	[32]
Alkali treatment combined with enzymatic hydrolysis and petroleum ether extraction	leaves	6.21	1.0	6.2	[33]

### 3.4.4. Thermo Gravimetric Analysis

The thermal stability properties of the purified gutta-percha were tested. As can be seen in Figure 11, the TG curve shows a thermal weight loss step, and the corresponding DTG curve shows only one distinct peak, indicating that the thermal-oxidative degradation reaction of gutta-percha is a one-step reaction, which is attributed to the degradation of the isoprene linkages [34]. The decomposition of gutta-percha began at around 300 °C, followed by a steep and pronounced weight loss step with increasing temperature, and the TG curve stabilized at around 500 °C, indicating that the decomposition of gutta-percha was complete. The maximum peak value of the DTG curve occurred at around 387.5 °C, indicating a maximum thermal degradation rate at this temperature. The main degradation process of gutta-percha occurred at 330–460 °C, which is consistent with that reported in other literature [9].

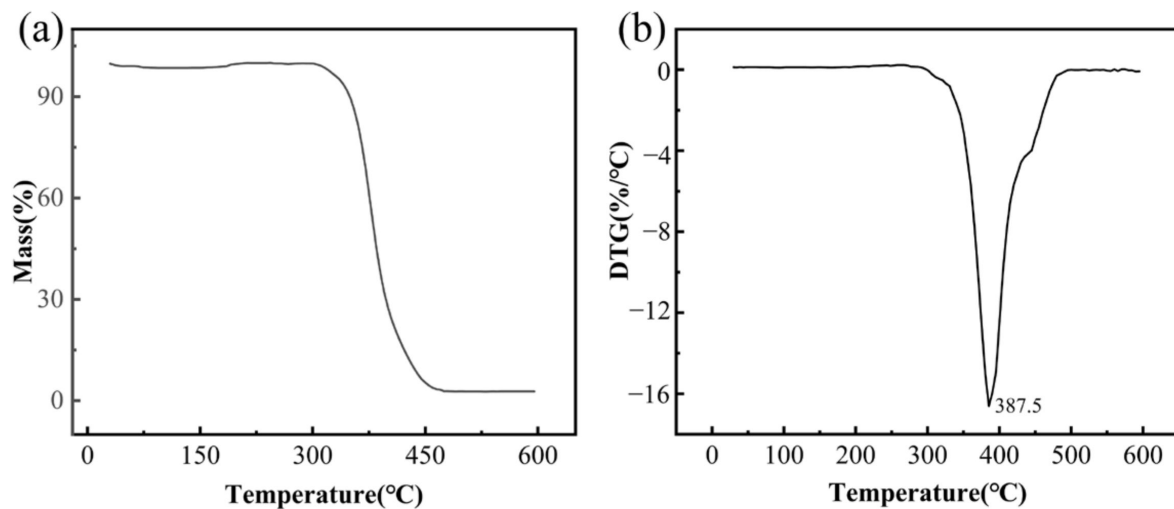


**Figure 11.** (a) TGA and (b) DTG curves of the purified gutta-percha.

#### 3.4.5. DSC Analysis

The crystallization behavior of purified gutta-percha was studied by DSC (Figure 12). It can be seen that there were two endothermic peaks in the process of heating, among which the absorption peak at 43.15 °C is the melting peak of  $\beta$ -crystal, and 58.78 °C is the melting peak of  $\alpha$ -crystal [7,34]. During the cooling process of gutta-percha, there was a sharp crystallization peak in the range of 20–25 °C, and the maximum crystallization rate temperature was 23.2 °C. The crystallinity of purified gutta-percha was 48.3%.

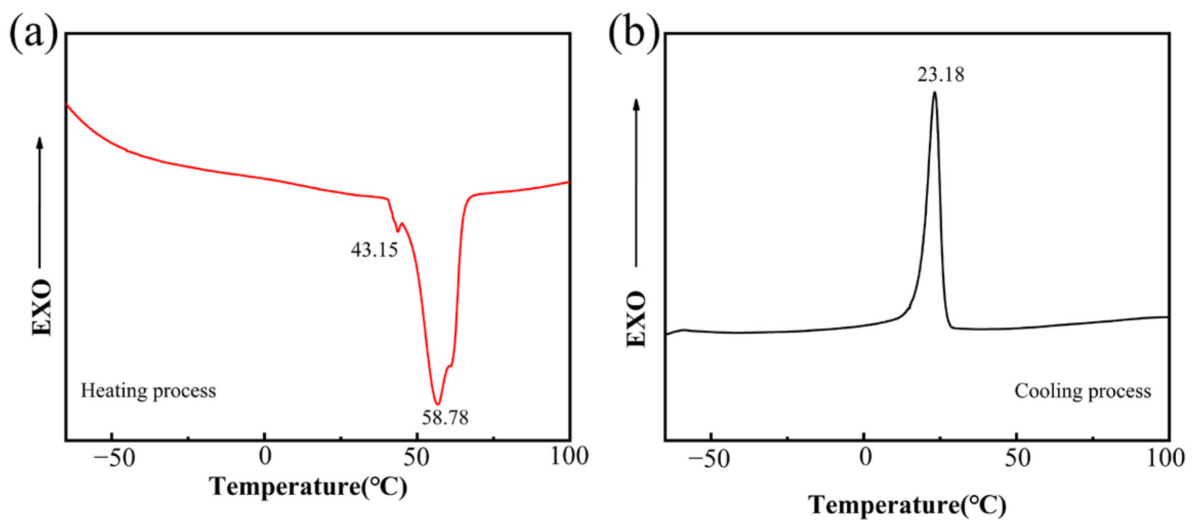


**Figure 12.** DSC curves (a) Heating process and (b) Cooling process of the purified gutta-percha.

#### 3.4.6. Mechanical Tensile Properties Analysis

Figure 13 shows the stress-strain curves of the gutta-percha extracted by the proposed method and by petroleum ether. It can be found that the tensile strength of the gutta-percha extracted by the proposed method was 26.5 Mpa and the elongation at break was 441.1%, while the tensile strength and elongation at break of the gutta-percha extracted by petroleum ether was 17.14 Mpa and 303.1%, indicating that the gutta-percha obtained by the proposed method showed better tensile properties.

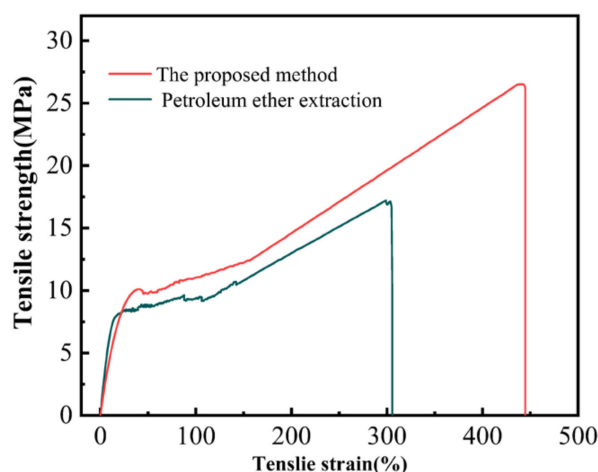


Figure 13. The stress-strain curves of gutta-percha.

#### 4. Conclusions

Gutta-percha in *E. ulmoides* is in solid form and does not flow automatically from plant tissues like hevea rubber, so it must be extracted by physical, chemical, or biological methods. In this study, specific enzymes were used to hydrolyze and destroy the plant tissues outside gutta-percha, and then ultrasound treatment and surfactant aqueous dispersion was used in turn to further remove the residual plant tissue debris, finally yielding gutta-percha with a purity of  $95.4 \pm 0.31\%$ , which retained its native filamentous structure and no chemical residues. The proposed method features a simple process and low production cost without needing any expensive instruments. Therefore, the method can be easily applied to the industry for the continuous large-scale production of high-purity, native state gutta-percha.

**Supplementary Materials:** The following supporting information can be downloaded at: <https://www.mdpi.com/article/10.3390/agriculture12070904/s1>, Ultrasonic stripping mechanism [35–37]; Aqueous phase dispersion mechanism of surfactant; Scheme S1. A micro-crack layer between gutta-percha and plant tissue debris; Figure S1. Gutta-percha in aqueous solution containing SDS. Table S1: Experimental design and results of response surface analysis for ultrasonic purification processes; Table S2: Analysis of variance (ANOVA) results of the regression equation for ultrasonic purification; Table S3: Experimental design and results of response surface analysis for surfactant purification processes; Table S4: ANOVA results of the regression equation for surfactant purification.

**Author Contributions:** Q.S.: Writing original draft, Validation. Y.H.: Data curation, Methodology, Investigation, Formal analysis. X.Z.: Investigation, Funding acquisition, Formal analysis, Supervision. Q.W.: Investigation, Formal analysis. H.T.: Funding acquisition, Project administration, Formal analysis, Conceptualization, Supervision, Writing—review & editing. All authors have read and agreed to the published version of the manuscript.

**Funding:** This work was financially supported by Guizhou Provincial Science and Technology Project (QKHJC-ZK[2022]Key015), the Project of National Key Research and Development Program (2017YFD0600702).

**Institutional Review Board Statement:** Not applicable.

**Informed Consent Statement:** Not applicable.

**Data Availability Statement:** Not applicable.

**Conflicts of Interest:** The authors declare no conflict of interest.

## References

1. Qi, X.; Zhang, J.H.; Zhang, L.Q.; Yue, D.M. Bio-based self-healing *Eucommia ulmoides* ester elastomer with damping and oil resistance. *J. Mater. Sci.* **2020**, *55*, 4940–4951. [[CrossRef](#)]
2. Wei, X.; Peng, P.; Peng, F.; Dong, J. Natural Polymer *Eucommia Ulmoides* Rubber: A Novel Material. *J. Agric. Food Chem.* **2021**, *69*, 3797–3821. [[CrossRef](#)]
3. Zhang, H.; Ma, C.; Sun, R.; Liao, X.; Wu, J.; Xie, M. Sustainable elastomer of triazolinedione-modified *Eucommia ulmoides* gum with enhanced elasticity and shape memory capability. *Polymer* **2019**, *184*, 121904. [[CrossRef](#)]
4. Xia, L.; Wang, Y.; Ma, Z.; Du, A.; Qiu, G.; Xin, Z. Preparation of epoxidized *Eucommia ulmoides* gum and its application in styrene-butadiene rubber (SBR)/silica composites. *Polym. Adv. Technol.* **2017**, *28*, 94–101. [[CrossRef](#)]
5. Wang, Y.; Liu, J.; Xia, L.; Shen, M.; Xin, Z.; Kim, J. Role of epoxidized natural *Eucommia ulmoides* gum in modifying the interface of styrene-butadiene rubber/silica composites. *Polym. Adv. Technol.* **2019**, *30*, 2968–2976. [[CrossRef](#)]
6. Banphakarn, N.; Yanpiset, K.; Banomyong, D. Shear bond strengths of calcium silicate-based sealer to dentin and calcium silicate-impregnated gutta-percha. *J. Investig. Clin. Dent.* **2019**, *10*, e12444. [[CrossRef](#)] [[PubMed](#)]
7. Zhang, B.-X.; Azuma, J.-I.; Takeno, S.; Suzuki, N.; Nakazawa, Y.; Uyama, H. Improvement of the rheological properties of trans-1,4-polyisoprene from *Eucommia ulmoides* Oliver by tri-branched poly(ricinoleic acid). *Polym. J.* **2016**, *48*, 821–827. [[CrossRef](#)]
8. Wang, Y.; Pei, X.Q.; Xia, L.; Zhang, Z.C.; Wang, Q.H.; Wang, T.M. Bio-based *Eucommia ulmoides* gum/low density polyethylene shape memory composites reinforced by zinc methacrylate. *Polym. Int.* **2021**, *70*, 1659–1667. [[CrossRef](#)]
9. Yang, H.H.; Peng, P.; Sun, Q.Q.; Zhang, Q.; Ren, N.; Han, F.P.; She, D. Developed carbon nanotubes/gutta percha nanocomposite films with high stretchability and photo-thermal conversion efficiency. *J. Mater. Res. Technol. JmrT* **2020**, *9*, 8884–8895. [[CrossRef](#)]
10. Kang, H.; Gong, M.; Xu, M.; Wang, H.; Li, Y.; Fang, Q.; Zhang, L. Fabricated Biobased *Eucommia Ulmoides* Gum/Polyolefin Elastomer Thermoplastic Vulcanizates into a Shape Memory Material. *Ind. Eng. Chem. Res.* **2019**, *58*, 6375–6384. [[CrossRef](#)]
11. Qi, X.; Xu, E.; Jia, M.; Zhang, J.; Zhang, L.; Yue, D. Bio-Based, Self-Crosslinkable *Eucommia ulmoides* Gum/Silica Hybrids with Body Temperature Triggering Shape Memory Capability. *Macromol. Mater. Eng.* **2021**, *306*, 2100370. [[CrossRef](#)]
12. Wang, Q.; Xiong, Y.; Dong, F. *Eucommia ulmoides* gum-based engineering materials: Fascinating platforms for advanced applications. *J. Mater. Sci.* **2021**, *56*, 1855–1878. [[CrossRef](#)]
13. Liu, X.; Wang, X.Z.; Kang, K.; Sun, G.T.; Zhu, M.Q. Review on extraction, characteristic, and engineering of the *Eucommia ulmoides* rubber for industrial application. *Ind. Crops Prod.* **2022**, *180*, 114733. [[CrossRef](#)]
14. Yang, F.; Hu, S.; Li, D.; Kang, H.; Fang, Q. Progress in Extraction Methods of *Eucommia Ulmoides* gum. *Polym. Mater. Sci. Eng.* **2020**, *36*, 177–182. [[CrossRef](#)]
15. Zhang, X.; Cheng, C.; Zhang, M.; Lan, X.; Wang, Q.; Han, S. Effect of alkali and enzymatic pretreatments of *Eucommia ulmoides* leaves and barks on the extraction of gutta percha. *J. Agric. Food Chem.* **2008**, *56*, 8936–8943. [[CrossRef](#)] [[PubMed](#)]
16. Tang, X.X.; Qiu, P.S.; Duan, Z.H.; Shang, F.F.; Tang, Q.; Mo, Z.Z.; Liu, Y. Optimization of Ultrasonic-Microwave Assisted Extraction of Dietary Fiber from Lotus Root by Response Surface Methodology. *Food Res. Dev.* **2019**, *40*, 132–139. [[CrossRef](#)]
17. Chen, H.T.; Shen, X.S. Optimization of ultrasound—Microwave assisted extraction of proanthocyanidin from brown rice by response surface methodology. *Sci. Technol. Food Ind.* **2018**, *39*, 186–191. [[CrossRef](#)]
18. Carbone, K.; Amoriello, T.; Iadecola, R. Exploitation of Kiwi Juice Pomace for the Recovery of Natural Antioxidants through Microwave-Assisted Extraction. *Agriculture* **2020**, *10*, 435. [[CrossRef](#)]
19. Unsal, M.; Isik-Gulsac, I.; Uresin, E.; Budak, M.S.; Ozgur-Buyuksakalli, K.; Sayar, A.; Aksoy, P.; Unlu, N.; Okur, O.; Sahin, H.; et al. Optimisation of biomass catalytic depolymerisation conditions by using response surface methodology. *Waste Manag. Res.* **2020**, *38*, 322–331. [[CrossRef](#)]
20. Wang, Y.; Wang, Y.W.; Xia, L.; Xin, Z.X. Extraction of EUG by Organic Phase-Aqueous Phase Method and Its Structure Characterization. *China Rubber Ind.* **2017**, *64*, 650–654.
21. Wu, M.F.; Liu, P.Y.; Wang, S.Y.; Zhong, C.; Zhao, X.H. Ultrasonic Microwave-Assisted Micelle Combined with Fungal Pretreatment of *Eucommia ulmoides* Leaves Significantly Improved the Extraction Efficiency of Total Flavonoids and Gutta-Percha. *Foods* **2021**, *10*, 2399. [[CrossRef](#)] [[PubMed](#)]
22. Qian, S.Y.; Zhang, C.; Zhu, Z.D.; Huang, P.P.; Xu, X.Q. White rot fungus *Inonotus obliquus* pretreatment to improve trans-1,4-polyisoprene extraction and enzymatic saccharification of *Eucommia ulmoides* leaves. *Appl. Biochem. Biotechnol.* **2020**, *192*, 719–733. [[CrossRef](#)] [[PubMed](#)]
23. Damas, J.; Remacle-Volon, G.; Deflandre, E. Further studies of the mechanism of counter irritation by turpentine. *Naunyn-Schmiedeberg's Arch. Pharmacol.* **1986**, *332*, 196–200. [[CrossRef](#)] [[PubMed](#)]
24. Nakazawa, Y.; Takeda, T.; Suzuki, N.; Hayashi, T.; Harada, Y.; Bamba, T.; Kobayashi, A. Histochemical study of trans-polyisoprene accumulation by spectral confocal laser scanning microscopy and a specific dye showing fluorescence solvatochromism in the rubber-producing plant, *Eucommia ulmoides* Oliver. *Planta* **2013**, *238*, 549–560. [[CrossRef](#)] [[PubMed](#)]
25. Zhang, C.-B.; Wang, L.; Yang, B.; Zhao, H.; Liu, G.-M.; Wang, D.-J. Stress-induced Solid-Solid Crystal Transition in Trans-1,4-polyisoprene. *Chin. J. Polym. Sci.* **2022**, *40*, 256–265. [[CrossRef](#)]
26. Mandelkern, L.; Quinn, F.A.; Roberts, D.E. Thermodynamics of Crystallization in High Polymers: Gutta Percha 1,2. *Rubber Chem. Technol.* **1956**, *29*, 1181–1194. [[CrossRef](#)]

27. Yue, P.P.; Leng, Z.J.; Bian, J.; Li, M.F.; Peng, F.; Sun, R.C. Fast and simple construction of composite films with renewable *Eucommia ulmoides* gum and Poly(epsilon-caprolactone). *Compos. Sci. Technol.* **2019**, *179*, 145–151. [[CrossRef](#)]
28. Zhang, J.; Xue, Z. A comparative study on the properties of *Eucommia ulmoides* gum and synthetic trans-1,4-polyisoprene. *Polym. Test.* **2011**, *30*, 753–759. [[CrossRef](#)]
29. Sun, Q.; Zhao, X.; Wang, D.; Dong, J.; She, D.; Peng, P. Preparation and characterization of nanocrystalline cellulose/*Eucommia ulmoides* gum nanocomposite film. *Carbohydr. Polym.* **2018**, *181*, 825–832. [[CrossRef](#)]
30. Guo, T.; Liu, Y.; Wei, Y.; Ma, X.; Fan, Q.; Ni, J.; Yin, Z.; Liu, J.; Wang, S.; Dong, Y.; et al. Simultaneous qualitation and quantitation of natural trans-1,4-polyisoprene from *Eucommia ulmoides* Oliver by gel permeation chromatography (GPC). *J. Chromatogr. B-Anal. Technol. Biomed. Life Sci.* **2015**, *1004*, 17–22. [[CrossRef](#)]
31. Cui, G.; Liu, Z.; Wei, M.; Yang, L. Turpentine as an alternative solvent for the extraction of gutta-percha from *Eucommia ulmoides* barks. *Ind. Crops Prod.* **2018**, *121*, 142–150. [[CrossRef](#)]
32. Ding, H.; Liu, H.; Yang, Y.; Zhu, J.; Li, S.; Jia, Z.; Sun, Z. Enhanced Gutta-Percha Production from *Eucommia ulmoides* Oliver via Steam Explosion. *J. Biobased Mater. Bioenergy* **2019**, *13*, 353–362. [[CrossRef](#)]
33. Zhu, M.-Q.; Wen, J.-L.; Zhu, Y.-H.; Su, Y.-Q.; Sun, R.-C. Isolation and analysis of four constituents from barks and leaves of *Eucommia ulmoides* Oliver by a multi-step process. *Ind. Crops Prod.* **2016**, *83*, 124–132. [[CrossRef](#)]
34. Yang, F.; Hu, S.; Wei, J.; Li, D.; Kang, H.; Fang, Q. Preparation of Liquid *Eucommia Ulmoides* Gum. *Polym. Mater. Sci. Eng.* **2020**, *36*, 32–39. [[CrossRef](#)]
35. Gabaldón-Leyva, C.A.; Quintero-Ramos, A.; Barnard, J.; Balandrán-Quintana, R.R.; Talamás-Abbud, R.; Jiménez-Castro, J. Effect of ultrasound on the mass transfer and physical changes in brine bell pepper at different temperatures. *J. Food Eng.* **2007**, *81*, 374–379. [[CrossRef](#)]
36. Soria, A.C.; Villamiel, M. Effect of ultrasound on the technological properties and bioactivity of food: A review. *Trends Food Sci. & Technol.* **2010**, *21*, 323–331. [[CrossRef](#)]
37. Umego, E.C.; He, R.; Ren, W.; Xu, H.; Ma, H. Ultrasonic-assisted enzymolysis: Principle and applications. *Process Biochem.* **2021**, *100*, 59–68. [[CrossRef](#)]